JMEPEG (2009) 18:287–298
DOI: 10.1007/s11665-008-9295-4

1059-9495/$19.00

Investigation on Pitting Corrosion of Nickel-Free and Manganese-Alloyed High-Nitrogen Stainless Steels

Xinqiang Wu, Yao Fu, Junbo Huang, Enhou Han, Wei Ke, Ke Yang, and Zhouhua Jiang

(Submitted December 26, 2007; in revised form June 30, 2008)

Pitting corrosion behavior of three kinds of nickel-free and manganese-alloyed high-nitrogen (N) stainless steels (HNSSs) was investigated using electrochemical and immersion testing methods. Type 316L stainless steel (316L SS) was also included for comparison purpose. Both solution-annealed and sensitization-treated steels were examined. The solution-annealed HNSSs showed much better resistance to pitting corrosion than the 316L SS in both neutral and acidic sodium chloride solutions. The addition of molybdenum (Mo) had no further improvement on the pitting corrosion resistance of the solution-annealed HNSSs. The sensitization treatment resulted in significant degradation of the pitting corrosion resistance of the HNSSs, but not for the 316L SS. Typical large size of corrosion pits was observed on the surface of solution-annealed 316L SS, while small and dispersed corrosion pits on the surfaces of solution-annealed HNSSs. The sensitization-treated HNSSs suffered very severe pitting corrosion, accompanying the intergranular attack. The addition of Mo significantly improved the resistance of the sensitization-treated HNSSs to pitting corrosion, particularly in acidic solution. The good resistance of the solution-annealed HNSSs to pitting corrosion could be attributed to the passive film contributed by N, Cr, and Mo. The sensitization treatment degraded the passive film by decreasing anti-corrosion elements and Cr-bearing oxides in the passive film.

Keywords corrosion resistance, high-nitrogen stainless steels, passive film, pitting corrosion, sensitization treatment

1. Introduction

High-nitrogen (N) alloyed stainless steels (HNSSs) have attracted much attention during past several decades due to their well-balanced combination of excellent mechanical properties and corrosion resistance. In recent years, nickel (Ni)-free HNSSs have been developed for purposes of saving resources, avoiding Ni allergy problems and fabricating non-magnetic materials, which may offer some interesting solutions in the fields of surgical cutting tools, implant materials, instruments for examination in strong magnetic fields, costume jewellery, and kitchen utensils.

N is usually regarded as an ideal element replacing partly or entirely Ni in Ni-saving stainless steels without damaging the mechanical properties and corrosion resistance (Ref 1, 2). The influence of N alloying on the corrosion properties of stainless steels has received much attention and a number of reviews have been focused on this topic in recent years (Ref 3-5). It is generally believed that N alloying may improve the local corrosion resistance of stainless steels (Ref 6-10). With an increase of N content, the resistance of stainless steels to pitting corrosion, crevice corrosion, and stress corrosion cracking has been improved remarkably, particularly for the HNSSs with combined additions of N and molybdenum (Mo). There has been extensive discussion in the previous literatures about effects of N or N-Mo synergism on corrosion properties and various mechanisms have been proposed. Typical mechanisms to explain the beneficial roles of N alloying on corrosion properties of stainless steels consist of theories of ammonia production (Ref 11, 12), surface enrichment (Ref 13-15), anodic segregation (Ref 16-18), salt film formation (Ref 19), and synergistic effects of N, Mo, and chromium (Ref 16, 20-22). However, there is still a fair amount of controversy regarding the independent and synergistic effects of N and Mo alloying on general corrosion or active dissolution (Ref 7, 23-25), passive film properties (Ref 25-27), pitting resistance (Ref 28-30), and stress corrosion cracking (Ref 31, 32). The related mechanisms are still under debate.

Manganese (Mn) increases N solubility and assists in stabilizing the austenitic microstructure as well as reduces cost by replacing Ni (Ref 33). Moreover, Mn unlike Ni is an essential trace element for the human body and is thus biocompatible. Mn, therefore, becomes another alternative alloying element in Ni-free HNSSs. However, Mn alloying seemed to be detrimental to corrosion resistance of N-bearing stainless steels. Our previous work has showed that high Mn alloying caused obvious degradation on the general and intergranular corrosion resistance of the HNSSs (Ref 34). It has also been reported that Mn alloying degraded the resistance of the HNSSs to localized corrosion (Ref 35-37).

The present work is to investigate the pitting corrosion behavior of three kinds of Ni-free and Mn-alloyed HNSSs as well as a 316L stainless steel (316L SS) using electrochemical

Xinqiang Wu, Yao Fu, Junbo Huang, Enhou Han, Wei Ke, and **Ke Yang**, State Key Laboratory for Corrosion and Protection, Institute of Metal Research, Chinese Academy of Sciences, 62 Wencui Road, Shenyang 110016, P.R. China; and **Zhouhua Jiang**, School of Materials and Metallurgy, Northeastern University, Shenyang 110004, P.R. China. Contact e-mail: xqwu@imr.ac.cn.

and immersion testing methods. Both the solution-annealed and sensitization-treated specimens were examined. The effects of Mo alloying on the pitting resistance of the HNSSs were investigated and the related mechanisms were discussed.

2. Experimental

Three kinds of Ni-free and Mn-alloyed HNSSs were used in the present work. All the steels are made by high-frequency vacuum refinement. The chemical compositions of the HNSSs are listed in Table 1. Type 316L SS was also included for comparison purpose. The specimens of $10 \times 10 \times 3$ mm for electrochemical tests and pitting corrosion investigations were machined from the hot rolled sheets. All the specimens were solution annealed at 1200 °C for 1 h in an argon protective atmosphere followed by water quenching. Sensitization treatments were performed for some specimens at a temperature of 650 °C for 2 h in an evacuated tube and water quenched. Electrolytic etching with 10% oxalic acid solution was used to reveal the microstructure in the present study.

Electrochemical measurements were made at ambient temperature in naturally aerated neutral solution of 3.5% NaCl and acidic solution of 0.5 M NaCl + 0.5 M H_2SO_4. Testing solutions were all prepared from analytical grade reagents and triply distilled water. The testing specimens were mounted in araldite and mechanically polished up to 1 μm with metallurgical papers and then rinsed with distilled water. Polarization curves were recorded using a PAR & EG&G potentiostatic Model 273 A workstation. A saturated calomel electrode (SCE) was used as a reference electrode and a platinum plate was used as a counter electrode. Tests were conducted at a potential scan rate of 20 mV/min starting from the potential value 250 mV more negative than the corrosion potential. Electrochemical impedance spectroscopy (EIS) measurements were performed using a Solartron 1287 Electrochemical Interface and a Solartron 1260 Frequency response analyzer. EIS measurements were conducted at open circuit potential (OCP) in a frequency domain from 0.01 Hz to 1000 kHz, with the excitation voltage amplitude of 10 mV.

Pitting corrosion rate and pitting corrosion morphologies were examined using immersion testing of polished specimens in a solution comprising 100 g $FeCl_3 \cdot 6H_2O$ and 900 mL 0.05 mol/L HCl. The testing temperature was 35 °C and the testing duration was 24 h. All the specimens for immersion tests were weighed with 0.00001 g sensitivity analytical balance before and after corrosion tests. The corrosion rate mpy, with units of mm/year, was calculated as follows.

$$\text{mpy} = \frac{\Delta W}{\rho S t} \times 24 \times 365 \qquad \text{(Eq 1)}$$

where ΔW is the weight loss of specimens with units of g, ρ is the density of the stainless steels with units of g/mm^3, S is the total corrosion area with units of mm^2, and t is the time of exposure with units of h.

After metallographic etching or pitting corrosion tests, the specimens were rinsed with deionized water and alcohol and then dried. The microstructural characteristics and pitting corrosion morphologies were examined using an optical microscopy (OM) and a scanning electronic microscope (SEM) equipped with an energy dispersive spectrum analyzer. The phase analysis was performed using an X-ray diffraction (XRD) analyzer. The passive film were examined and analyzed by X-ray photoelectron spectroscopy (XPS).

3. Results

3.1 Microstructure

Figure 1 shows optical morphologies of microstructure of solution-annealed and sensitization-treated HNSSs and 316L SS used in the present study. It is clear that all the solution-annealed steels consisted of γ grains with typical twins (Fig. 1a, c, and e). The HNSS B and HNSS C showed very similar microstructural characteristics due to their similar chemical compositions. However, the sensitization treatment resulted in significant change of microstructure, particularly in the areas of grain boundary (Fig. 1b, d, and f). After electrolytic metallographic etching with 10% oxalic acid solution, the Mo-free HNSS A suffered severe attack along the grain boundaries (Fig. 1b). Observed at high magnification, cankerous attack patterns appeared frequently along the grain boundaries (Fig. 2a). The Mo-bearing HNSS B and HNSS C showed a relatively slight intergranular attack, but discontinuous attack was also observed along the grain boundaries (Fig. 1d). Observed at high magnification, such discontinuous attack was found to be composed of corrosion pits along the grain boundaries (Fig. 2b). Very fine step-like patterns could be observed inside these intergranular pits (Fig. 2c), seemingly suggesting that a step-like dissolution mechanism dominates the formation of the intergranular pits. For the 316L SS, continuous intergranular attack appeared on the specimen surface (Fig. 1f). Observed at high magnification, very narrow and continuous corrosion ditches appeared along the grain boundaries (Fig. 2d). The above results revealed that the sensitization treatments caused significant degradation of corrosion resistance of grain boundaries of the HNSSs and 316L SS. The addition of Mo, to some extent, improved the corrosion resistance of the HNSSs. In addition, it should be noted that the twin boundaries in the HNSSs and 316L SS showed little attack after electrolytic metallographic etching (Fig. 2a, b, and d), suggesting that the twin boundaries in the stainless steels inhere in much better corrosion resistance than the grain boundaries.

XRD analysis of the solution-annealed and sensitization-treated HNSSs and 316L SS indicated that no other peaks

Table 1 Chemical compositions of the steels used in the present study

Steels	Cr	Ni	Mn	Mo	N	Si	C	S	P	Al	Fe
HNSS A	19.8	…	18.4	…	0.82	…	0.04	0.012	0.015	0.02	Bal.
HNSS B	19.07	…	18.84	2.20	0.77	…	0.043	0.012	0.015	0.02	Bal.
HNSS C	18.4	…	15.8	2.19	0.66	0.24	0.04	0.005	0.017	0.02	Bal.
316L SS	16.4	10.2	1.02	2.36	…	0.40	0.019	0.06	0.033	…	Bal.

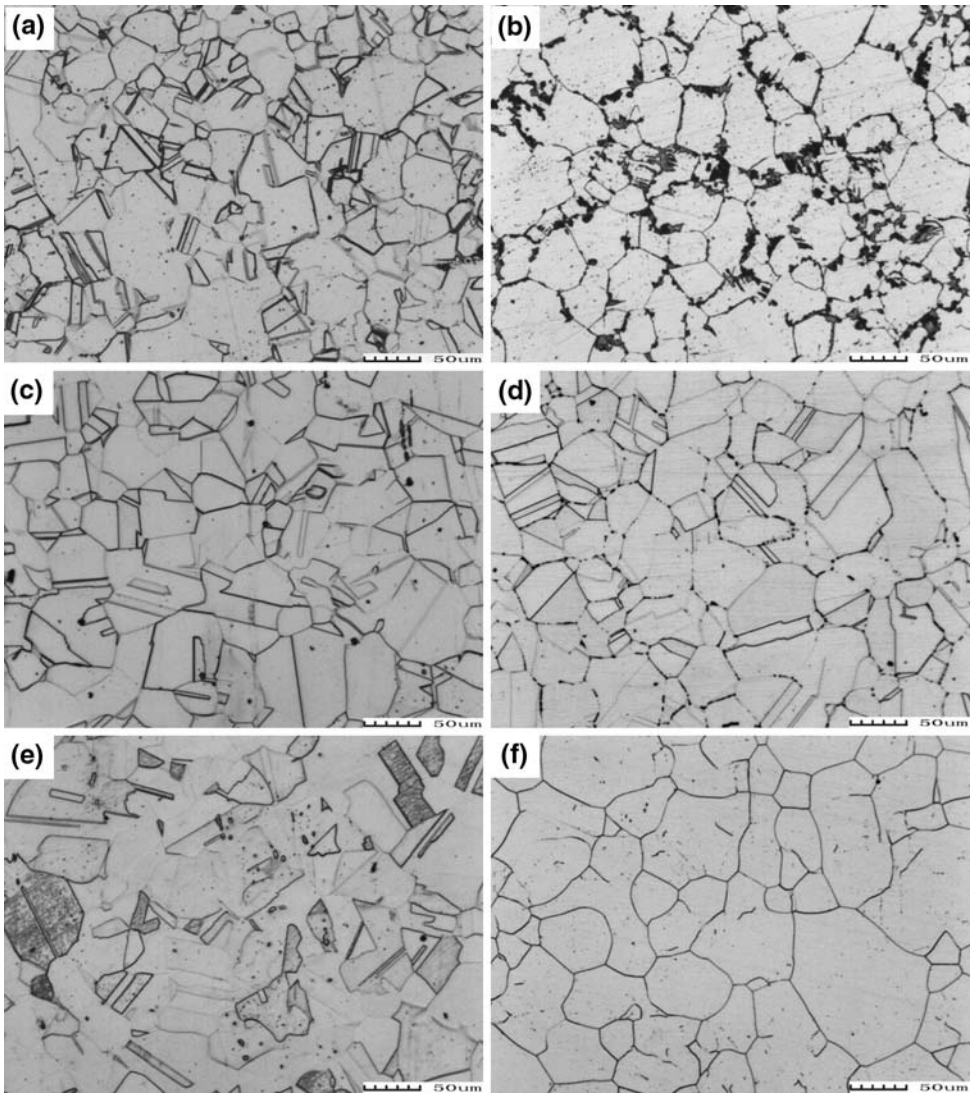

Fig. 1 OM morphologies of microstructure of solution annealed (a, c, e) and sensitization treated (b, d, f) of stainless steels used presently. (a, b) HNSS A, (c, d) HNSS C, and (e, f) 316L SS

except for the ones corresponding to γ phase appeared on the diffraction spectrum (Fig. 3), suggesting that the sensitization treatment in the present study do not induce any detectable precipitation in the steels, although it certainly caused degradation of corrosion resistance of grain boundaries of the HNSSs and 316L SS (Fig. 2).

3.2 Electrochemical Tests

Figure 4 shows polarization curves of the solution-annealed HNSSs and 316L SS in neutral 3.5% NaCl solution. The HNSSs showed much better pitting corrosion resistance than the 316L SS in NaCl solution. The pitting potentials of the HNSSs appeared very close to each other, irrespective of the Mo and N contents in the steels. The Mo-bearing HNSS B and HNSS C had very similar polarization behavior due to their similar chemical compositions. The passive current density of the Mo-free HNSS A was only a little higher than that of the other two Mo-bearing HNSSs, which could be attributed to beneficial effect of Mo on the stability of the passive film (Ref 31, 38-42). It should be noted that the 316L SS had no obvious passive region on the polarization curve, seemingly suggesting that active dissolution dominate the corrosion process of the 316L SS in neutral NaCl solution. Figure 5 shows polarization curves of the sensitization-treated HNSSs and 316L SS in neutral 3.5% NaCl solution. The sensitization treatment had obvious influence on the corrosion behavior of the HNSSs. For the Mo-free HNSS A, the passive region on the polarization curve almost disappeared. The active dissolution current density increased rapidly (Fig. 5a). For the Mo-bearing HNSS B and HNSS C, the passive current density of the sensitization-treated specimens was about 10 times that of the solution-treated specimens (Fig. 5b and c). However, the sensitization treatment seemed to have no influence on the pitting potentials of the sensitization-treated Mo-bearing HNSSs. For the 316L SS, both the solution-annealed and sensitization-treated specimens showed quite similar polarization behavior (Fig. 5d).

Figure 6 shows polarization curves of the solution-annealed HNSSs and 316L SS in 0.5 M NaCl + 0.5 M H_2SO_4 solution.

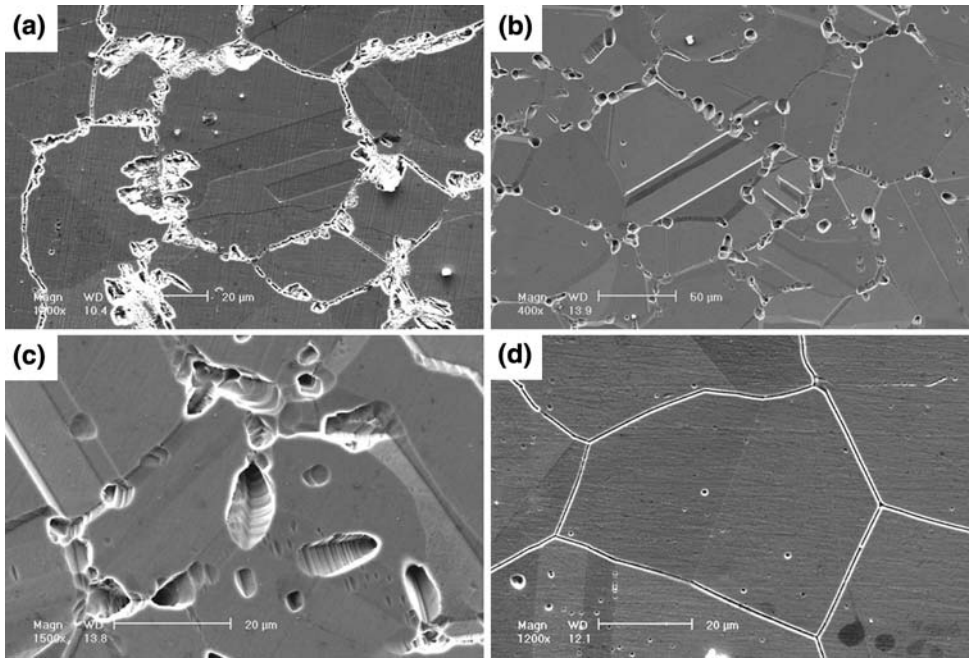

Fig. 2 SEM morphologies of microstructure of sensitization-treated stainless steels. (a) HNSS A, (b) HNSS C, (c) high magnification morphology of (b), and (d) 316L SS

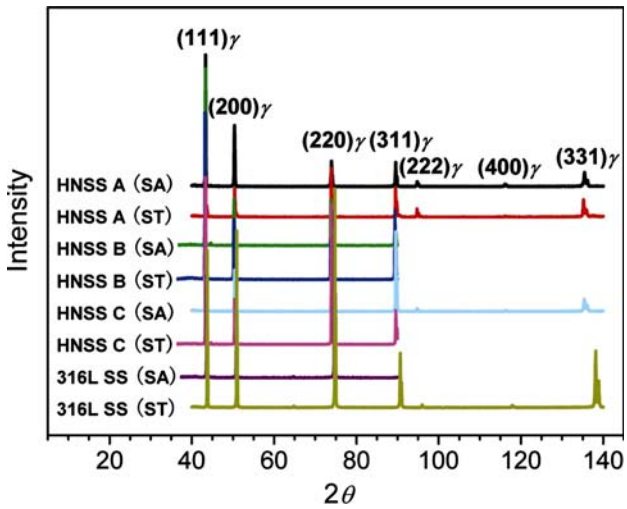

Fig. 3 XRD analysis of the solution-annealed (SA) and sensitization-treated (ST) HNSSs and 316L SS

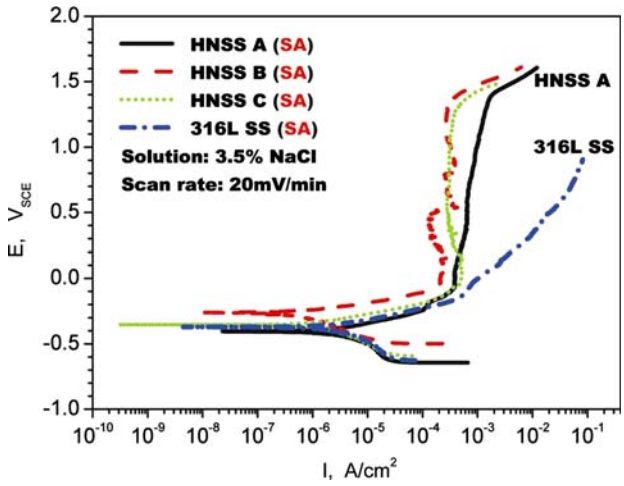

Fig. 4 Polarization curves of solution-annealed (SA) HNSSs and 316L SS in 3.5% NaCl solution

In the acidic solution, all the steels showed typical passivation. Moreover, the secondary passivation was observed for the HNSSs. The HNSSs had a much wider passive potential range compared to the 316L SS. The pitting potentials of the HNSSs were about 1 V higher than that of the 316L SS. However, the passive current density for all the steels appeared similar. It should be noted that the critical current density for passivation of the HNSSs was much higher than that of the 316L SS. After sensitization treatment, the corrosion resistance of the Mo-free HNSS A degraded significantly (Fig. 7a). The pitting potential of the sensitization-treated specimen was about 1.5 V lower than that of the solution-annealed one. The passive potential range on the polarization curve also became very narrow. The passive current density of the sensitization-treated specimen was about 10 times that of the solution-annealed one. For the Mo-bearing HNSS B, the polarization behavior of the sensitization-treated and solution-annealed specimens appeared similar except that the sensitization-treated specimen showed a larger passive current density than that of the solution-annealed one (Fig. 7b). The sensitization treatment showed little influence on the polarization behavior of the 316L SS (Fig. 7c).

Figure 8 shows EIS testing results of the solution-annealed and sensitization-treated HNSSs and 316L SS in neutral 3.5% NaCl solution. Impedance values and phase angle values were plotted in the Bode plot format in order to distinguish clearly the resistive and capacitive regions. Impedance values at the frequency $f \rightarrow 0$ give the sum of the polarization resistance

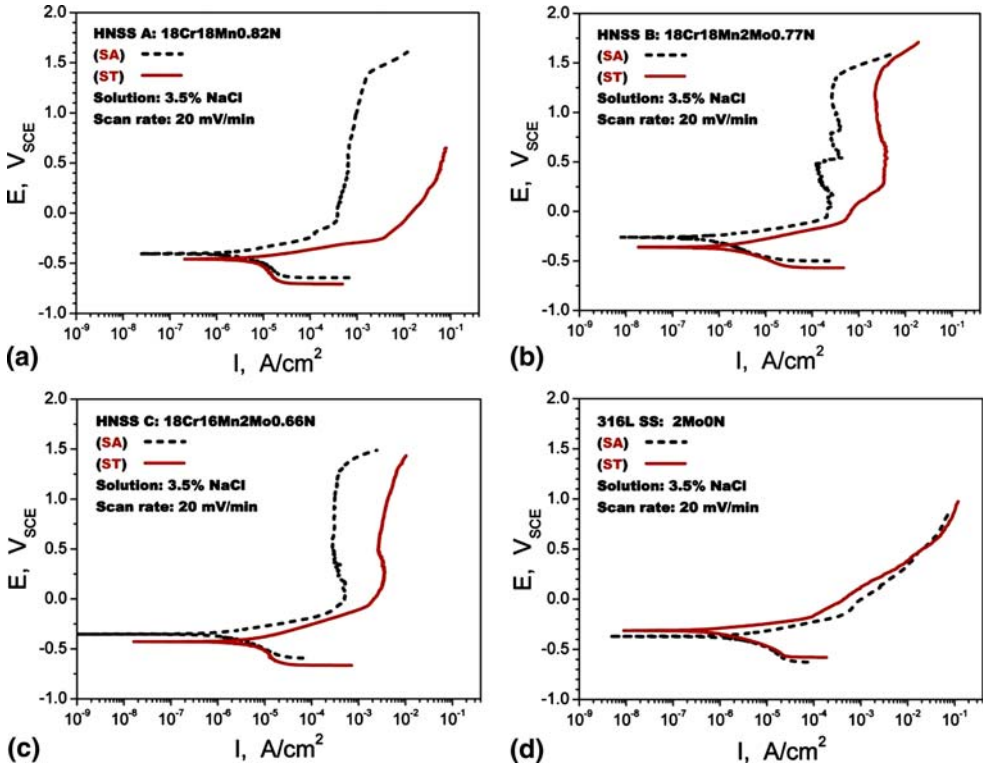

Fig. 5 Polarization curves of sensitization-treated (ST) HNSSs and 316L SS in 3.5% NaCl solution. (a) HNSS A, (b) HNSS B, (c) HNSS C, and (d) 316L SS

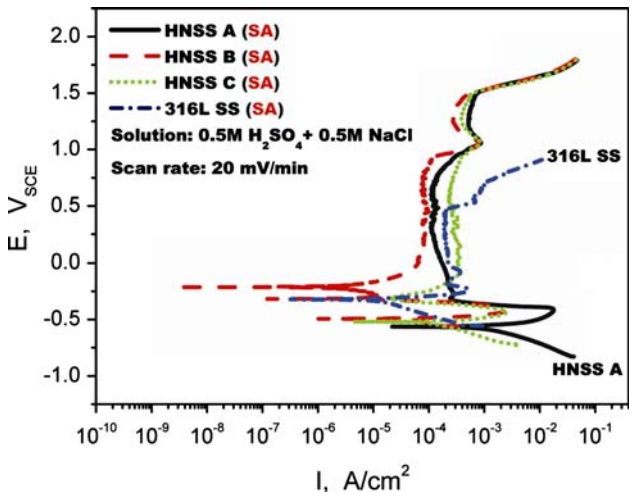

Fig. 6 Polarization curves of solution-annealed HNSSs and 316L SS in 0.5 M NaCl + 0.5 M H_2SO_4 solution

across the metal/solution interface R_p and the solution resistance R_{sol}. It was found that the solution-annealed HNSSs had relatively large impedance values ($f \rightarrow 0$) in comparison with the sensitization-treated steels, while the impedance values of the solution-annealed and sensitization-treated 316L SS almost kept a same level (Fig. 8a). In particular, the impedance values for both the solution-annealed and sensitization-treated HNSS B (Mo bearing) obtained at OCP were about 2-3 times that for the HNSS A (Mo free), indicating a higher value of R_p due to the Mo alloying. The phase angle plots indicate the nature of the film and its protectiveness, qualitatively. Generally, a broader capacitive loop indicates the formation of a more stable and protective film (Ref 43). In the present work, the capacitive loops observed at OCP for all the steels showed only a single time constant (Fig. 8b). The capacitive loops tended to become narrow for the sensitization-treated HNSSs (particularly for the Mo-free HNSS A), but not for the 316L SS. This suggested that the sensitization treatment used presently causes sure degradation on film stability of the HNSSs, especially for the Mo-free HNSS A. Nyquist plots showed depressed semicircle at high frequencies, attributed to the typical charge-transfer-dominated process, with some diffusion control (Fig. 8c), which was believed to be due to the film formation coupled with the restricted diffusion process (Ref 44, 45). It can be also seen from the Nyquist plots that the polarization resistance R_p of the sensitization-treated HNSSs were much lower than that of the solution-annealed steels.

3.3 XPS Analysis of Passive Film

Figure 9 shows distribution of the concentration of N, O, Cr, and Mo along the depth of the passive film in neutral 3.5% NaCl solution. It is clear that N, O, and Cr were rich in the surface layer of the passive film and their concentration decreased with the depth from the surface, while Mo, to some extent, was depleted in comparison with the matrix. The concentration of N, O, Cr, and Mo in the passive film of the solid-annealed HNSS was higher than that of the sensitization-treated one. Table 2 shows the oxides in surface, middle, and inner layers of the passive film. All the oxides were identified according to the binding energy of the elements within the passive film. It was found that the passive film of the solution-annealed HNSS

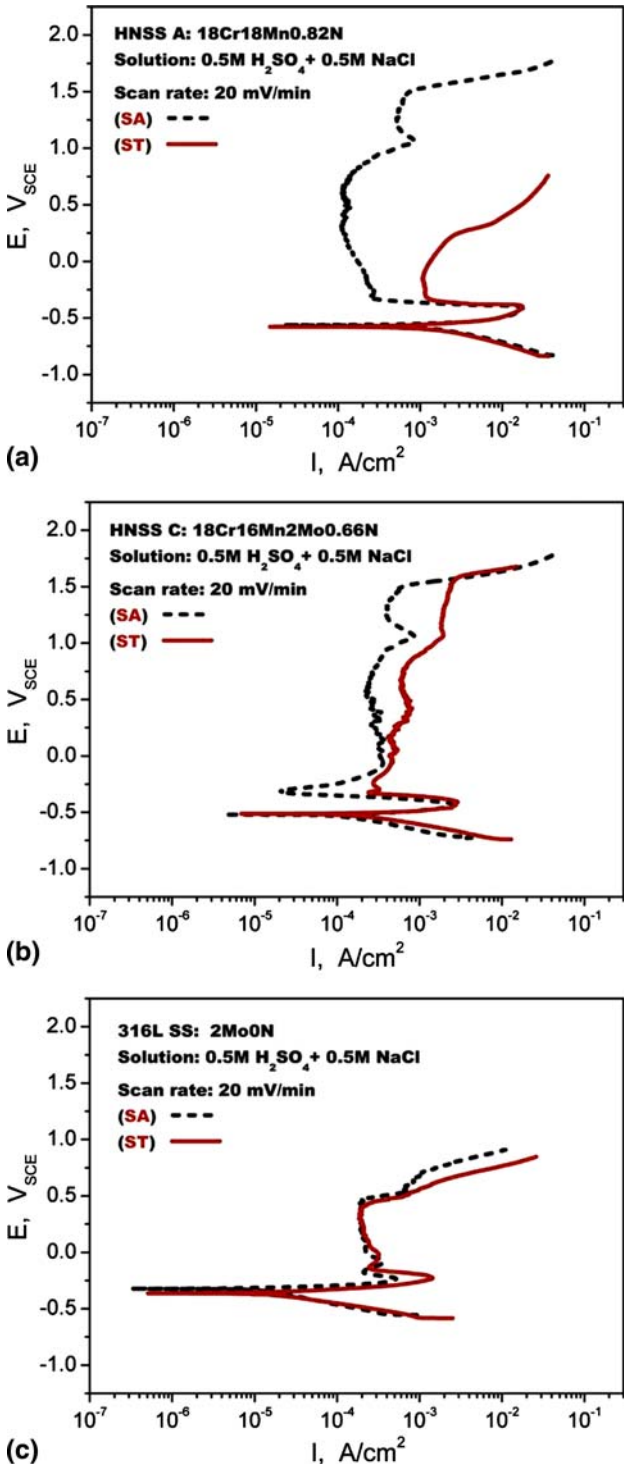

Fig. 7 Polarization curves of sensitization-treated HNSSs and 316L SS in 0.5 M NaCl + 0.5 M H_2SO_4 solution. (a) HNSS A, (b) HNSS C, and (c) 316L SS

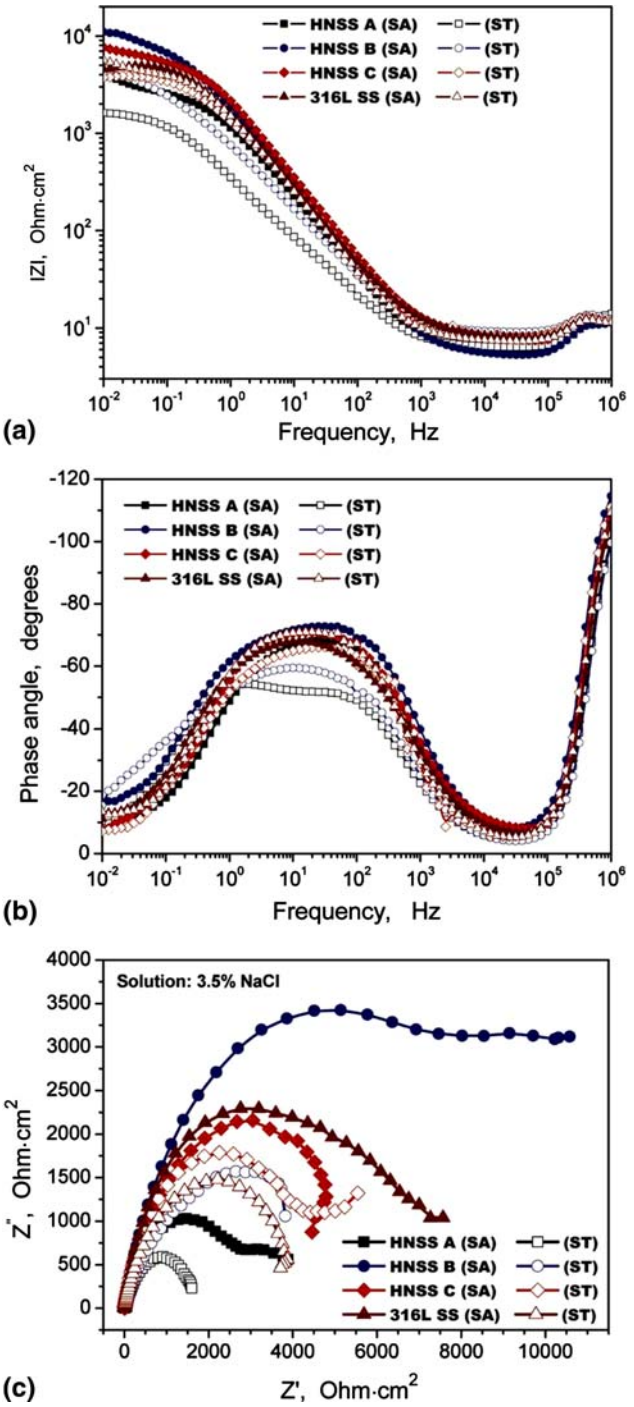

Fig. 8 EIS testing results of solution-annealed and sensitization-treated HNSSs and 316L SS in 3.5% NaCl solution. (a) Impedance plots, (b) phase angle plots, and (c) Nyquist plots

contained more oxides than that of the sensitization-treated one. Cr- and Mn-bearing oxides appeared in the middle and inner layers of the passive film of the solution-annealed HNSS, while no Cr-bearing oxides were detected in the middle and inner layers of the passive film in the sensitization-treated HNSS.

3.4 Pitting Corrosion Tests

Figure 10 shows corrosion rate of the solution-annealed and sensitization-treated HNSSs and 316L SS in a solution comprising 100 g $FeCl_3 \cdot 6H_2O$ and 900 mL 0.05 mol/L HCl at 35 °C. The 316L SS had the largest corrosion rate among all the solution-annealed steels, in good agreement with the previous electrochemical testing results shown in Fig. 4 and 6. The Mo-bearing HNSSs showed better corrosion resistance

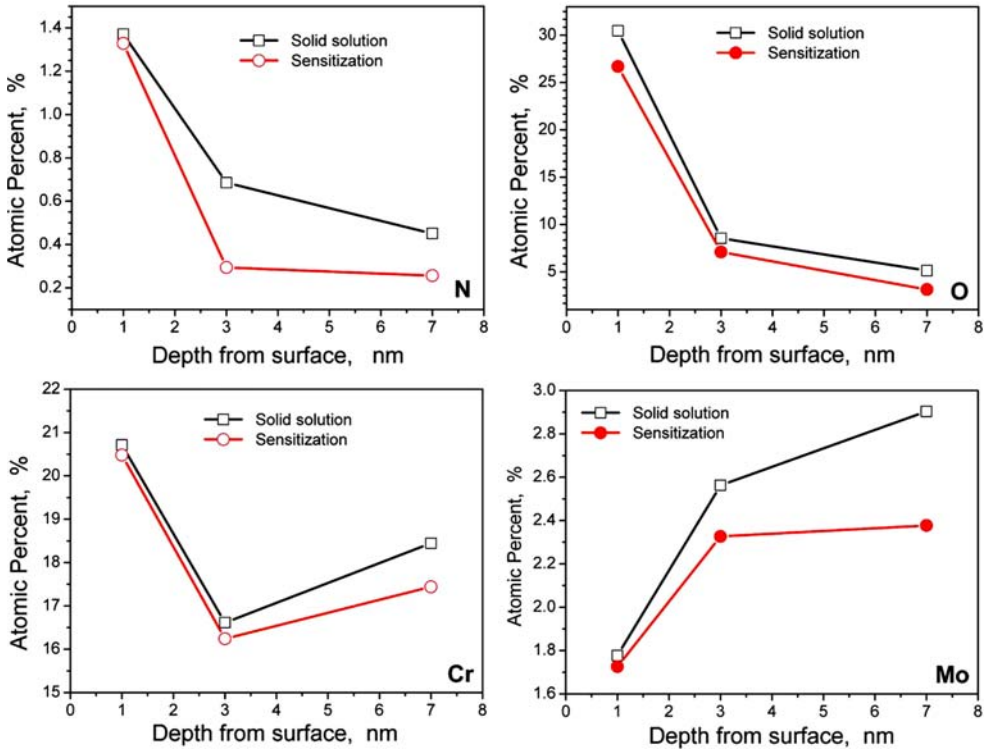

Fig. 9 Distribution of the concentration of N, O, Cr, and Mo along the depth of the passive film in neutral 3.5% NaCl solution

Table 2 Oxides in surface, middle, and inner layers of passive film in 3.5% NaCl solution

Specimens	Surface layer, 1 nm	Middle layer, 3 nm	Inner layer, 7 nm
Solution annealed	Cr_2O_3	CrO_x	CrO_x
	Fe_3O_4	Fe_3O_4	Fe_3O_4
	Mn_2O_3	MnO	MnO
Sensitization treated	CrO_x	Fe_3O_4	Fe_3O_4
	Fe_3O_4	MnO	
	MnO		

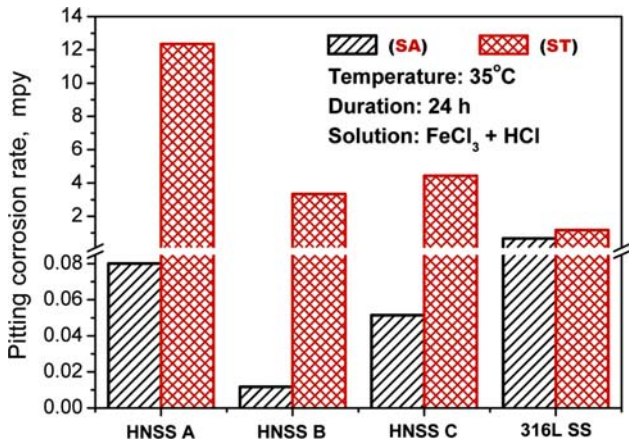

Fig. 10 Pitting corrosion rate of solution-annealed and sensitization-treated HNSSs and 316L SS in a solution comprising 100 g $FeCl_3 \cdot 6H_2O$ and 900 mL 0.05 mol/L HCl

compared to the Mo-free steel. The corrosion rate of solution-annealed Mo-free HNSS A was about 6-7 times that of the Mo-bearing HNSS B, although the former had the highest N content. The sensitization treatment resulted in significant degradation on corrosion resistance of the HNSSs. The corrosion rate of the sensitization-treated HNSSs was much higher than that of the 316L SS. For the Mo-free HNSS A, the corrosion rate of the sensitization-treated specimen was about 150 times that of the solution-annealed one. Even for the Mo-bearing HNSS B and HNSS C, an obvious increase in corrosion rate could be also observed for the sensitization-treated specimens. However, the sensitization-treated 316L SS specimen showed only a slight increase in corrosion rate compared to the solution-treated one, coinciding well with the previous electrochemical testing results.

Figure 11 shows pitting corrosion morphologies of the solution-annealed HNSSs and 316L SS in a solution comprising 100 g $FeCl_3 \cdot 6H_2O$ and 900 mL 0.05 mol/L HCl at 35 °C. For the HNSSs, lots of small and dispersed corrosion pits appeared on the specimen surfaces (Fig. 11a-c). There was no obvious difference in the initiation sites, size, and distribution of pits among the HNSSs. However, typical large size of pits except for many small ones appeared on the 316L SS specimen surface (Fig. 11d). Figure 12 shows pitting corrosion morphologies of sensitization-treated HNSSs and 316L SS. The sensitization-treated Mo-free HNSS A suffered severe corrosion. The original surface of the polished specimen had been damaged completely (Fig. 12a). Relatively slight corrosion damage was found on the specimen surfaces of the sensitization-treated HNSS B and HNSS C. Lots of large size of corrosion pits appeared on the specimen surfaces, relatively deep pits were predominantly developed along the grain boundaries (Fig. 12b and c). It should be noted that typical intergranular attack also

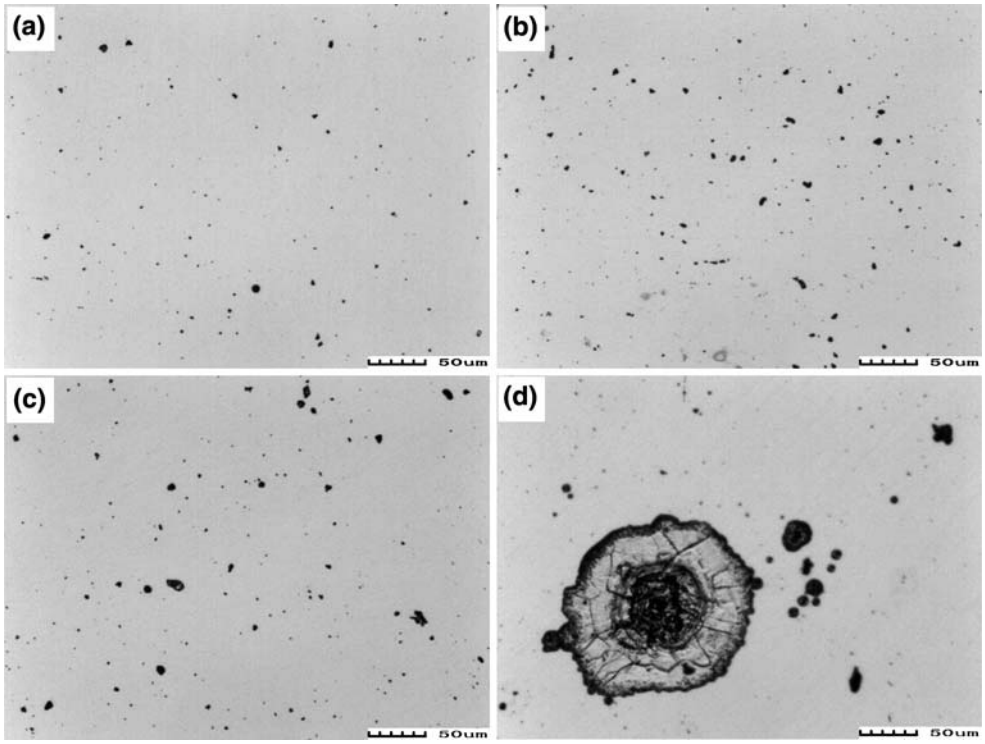

Fig. 11 OM morphologies of pitting corrosion of solution-annealed HNSSs and 316L SS in a solution comprising 100 g $FeCl_3 \cdot 6H_2O$ and 900 mL 0.05 mol/L HCl, temperature: 35 °C, duration: 24 h. (a) HNSS A, (b) HNSS B, (c) HNSS C, and (d) 316L SS

took place accompanying with the pitting corrosion. The intergranular attack was found to initiate frequently from the corrosion pits along the grain boundaries (Fig. 12d). For the sensitization-treated 316L SS, typical round pits were observed on the specimen surface (Fig. 12e). Also, quite large size of corrosion pits appeared on the specimen surface (Fig. 12f), just as the solution-annealed specimen (Fig. 11d). No intergranular attack could be found on the specimen surface of the sensitization-treated 316L SS.

4. Discussion

In the present work, according to the electrochemical testing results, the HNSSs showed a better pitting corrosion resistance in both neutral and acidic NaCl solutions in comparison with the 316L SS. The pitting potentials of the solution-annealed HNSSs were much higher than that of the 316L SS (Fig. 4 and 6), suggesting that the combined addition of N and Mn replacing Ni did not degrade the pitting corrosion resistance of stainless steels. This is believed to be mainly due to the high N alloying in the HNSSs. There is generally agreement that N alloying improves the pitting corrosion resistance of austenitic stainless steels, increasing the pitting potential and decreasing the corrosion rate in aqueous chloride solutions (Ref 26-28). The beneficial roles of N are usually attributed to that N can be concentrated on metal and oxidized surfaces to produce ammonium ions on the metal surface, and furthermore it can combine with Mo to form a more stable and dense passive film, thereby enhancing the corrosion resistance of stainless steels. Various N-related mechanisms have been discussed and proposed. The details could be found in the section ''Introduction.''

It should be noted that all the solution-annealed HNSSs showed very similar polarization behavior in both neutral and acidic NaCl solutions, although different N and Mo contents in these steels. All the solution-annealed HNSSs showed very similar pitting potentials, which were much higher than that of the 316L SS. Only a slight difference was observed on the passive current density among the steels (Fig. 4 and 6). This suggested that N alloying played a key role on the pitting corrosion resistance of the solution-annealed HNSSs, while the addition of Mo seemed to generate no further improvement on the pitting corrosion resistance. Moreover, the N content change from 0.66 wt.% (HNSS C) to 0.82 wt.% (HNSS A) seemed to have little influence on the pitting corrosion resistance of the solution-annealed HNSSs. However, the pitting corrosion tests of the HNSSs in a solution comprising 100 g $FeCl_3 \cdot 6H_2O$ and 900 mL 0.05 mol/L HCl solution showed that there was some difference in corrosion rate among the HNSSs (Fig. 10). The solution-annealed Mo-bearing HNSSs (HNSS B and C) had a lower corrosion rate than the Mo-free steel (HNSS A), indicating that Mo played a beneficial role on the corrosion resistance of the HNSSs. The difference between the electrochemical and immersion testing results may be due to the different testing methods. For the immersion tests with the duration of 24 h, although the pitting corrosion was dominant, it was believed that the general corrosion and/or intergranular attack also made some contribution to the corrosion rate. In this context, the corrosion rate calculated from the weight loss results of immersion tests was not a real indication of the resistance of the HNSSs to pitting corrosion. Mo alloying has been reported to have a beneficial effect on the resistance of the HNSSs to general and intergraunlar corrosion (Ref 34). As a result, the present immersion tests showed that Mo-bearing HNSSs had a better corrosion resistance than the

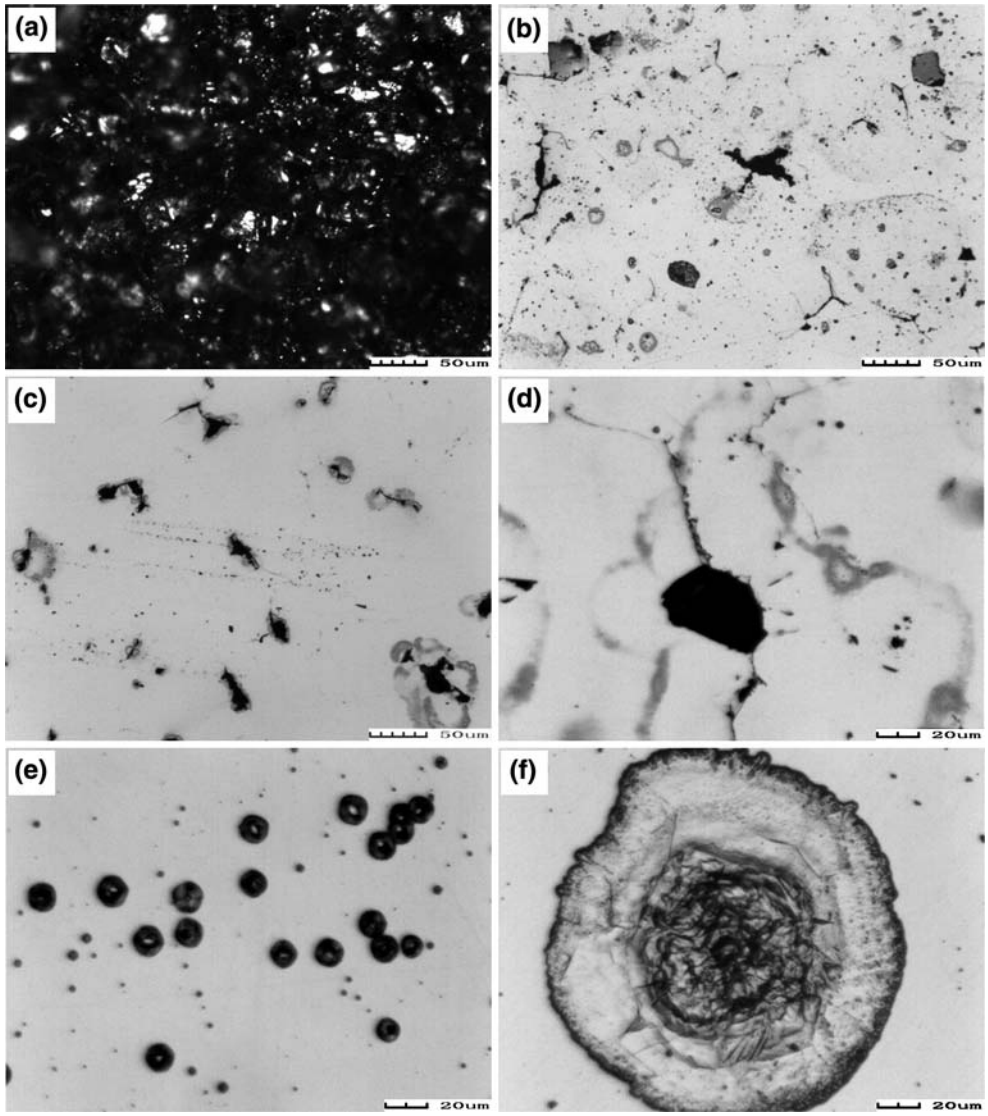

Fig. 12 OM morphologies of pitting corrosion of sensitization-treated HNSSs and 316L SS in a solution comprising 100 g $FeCl_3 \cdot 6H_2O$ and 900 mL 0.05 mol/L HCl, temperature: 35 °C, duration: 24 h. (a) HNSS A, (b) HNSS B, (c) HNSS C, (d) high-magnification morphology of pits on HNSS C specimen surface, (e) 316L SS, and (f) high-magnification morphology of pits on 316L SS specimen surface

Mo-free steel. In addition, it should be noted that the corrosion rates of the solution-annealed HNSSs were rather small (about 10^{-2} mpy in magnitude) and were much less than that of the 316L SS. Only small and dispersed corrosion pits were observed on the specimen surfaces of the HNSSs (Fig. 11a-c) in comparison with typical large corrosion pits that appeared on the 316L SS specimen surface (Fig. 11d). This suggested that the HNSSs appeared much less susceptible to the pitting corrosion in chloride solutions than the 316L SS, agreeing well with the previous electrochemical testing results.

The effect of N alloying on active dissolution of stainless steels is still under discussion. Much early work has noted that N alloying reduces the critical current density for passivation and general corrosion rate in concentrated reducing acids containing chlorides (Ref 16, 18, 24). However, N has also been reported to have a negligible effect on the active peak for Mo-bearing austenitic stainless steels in acidic NaCl solution (Ref 25) and Cr-Ni steels in sulfuric acid (Ref 7). It was also found that increasing the N content in duplex stainless steels caused an increase in the critical current density for passivation (Ref 46). In the present study, it was found that critical current density for passivation of the HNSSs in acidic NaCl solution was much higher than that of the 316L SS, particularly for the Mo-free HNSS A with the highest N content. The addition of Mo in the HNSSs, to some extent, resulted in a decrease of the critical current density for passivation. Such a large critical current density is believed to be due to the combined effects of Mn and N in the present HNSSs. Mn has been found to have negative effects on corrosion resistance of stainless steels due to its strong chemical activity. The Mn-rich areas or Mn-rich phases in stainless steels are easy to lose their electrons and to become anodes in an electrochemical reaction system in aggressive solutions. This thus promotes the anodic dissolution of stainless steels. In addition, N has frequently been reported to accelerate the anodic dissolution of iron in acidic solution (Ref 5, 47-49), also to promote the selective dissolution of iron from stainless steels (Ref 26, 46). As a result, the HNSSs with combined addition of high Mn and N showed higher peaks of

critical current density in comparison with the 316L SS. The addition of Mo lowered the critical current density for passivation of the HNSSs in acidic NaCl solution, which may be due to beneficial effect of Mo on improving general corrosion resistance of the HNSSs (Ref 34).

The sensitization treatment used in the present work caused significant degradation on pitting corrosion resistance of the HNSSs in both neutral and acidic NaCl solutions. For the Mo-free HNSS A, no typical passivation was observed for the sensitization-treated specimen in neutral NaCl solution. The specimen seemed to suffer continuous active dissolution (Fig. 5a). In acidic NaCl solution, the pitting potential decreased remarkably and the passive potential range became narrow for the sensitization-treated specimen, while the passive current density showed an increase by almost one order of magnitude (Fig. 7a), indicating significant degradation on corrosion resistance. The Mo alloying significantly improved the corrosion resistance of the sensitization-treated HNSSs. The pitting potential and the passive potential range of the sensitization-treated Mo-bearing HNSSs (HNSS B and C) in both neutral and acidic NaCl solutions kept almost the same as the solution-annealed ones (Fig. 5b, c and 7b). However, the passive current density of the sensitization-treated specimens showed an increase by almost one order of magnitude in neutral NaCl solution (Fig. 5b and c). Such an increase in the passive current density was not so obvious in the acidic NaCl solution (Fig. 7b), suggesting that the roles of Mo on improving the properties of passive film or corrosion resistance of the HNSSs appeared more effective in the acidic environments than in the neutral environments. For the 316L SS, the sensitization treatment showed little influence on its corrosion resistance in both neutral and acidic NaCl solution (Fig. 5d and 7c). The EIS results agreed well with the polarization testing results. All the solution-annealed HNSSs had relatively large impedance values in comparison with the sensitization-treated steels in the Bode plots, while the impedance values of the solution-annealed and sensitization-treated 316L SS almost kept a same level (Fig. 8a). The capacitive loops in the phase angle plots tended to become narrow for the sensitization-treated HNSSs, but not for the 316L SS. Both the solution-annealed and sensitization-treated Mo-bearing HNSSs showed larger impedance values and relatively narrow capacitive loops than the Mo-free steel. These results suggested that the sensitization treatment used presently caused sure degradation on film stability of the HNSSs, while the addition of Mo, to some extent, improved the nature of film and its protectiveness. This has been proved by the XPS results shown in Fig. 9 and Table 2. The concentration of anti-corrosion elements such as N, Mo, and Cr in the passive film of the sensitization-treated HNSSs decreased in comparison with that of the solution-annealed steels. Moreover, there were more oxides in the passive film of the solution-annealed HNSSs, particularly Cr-bearing oxides appearing in the middle and inner layers of the passive film. This is believed to improve the stability and protectiveness of the passive film of the solution-annealed HNSSs. In addition, the sensitization treatment seemed to have little influence on the film stability and protectiveness of the 316L SS according to the present polarization and EIS results.

The susceptibility of the HNSSs to the sensitization treatment can also be indicated by the results of the immersion tests in the $FeCl_3$ + HCl solution. A rapid increase in corrosion rate was observed for the sensitization-treated HNSSs, but not for the 316L SS (Fig. 10). The Mo-bearing HNSS B and C had lower corrosion rates compared to the Mo-free HNSS A. The corrosion rate of the sensitization-treated HNSSs was much higher than that of the 316L SS. Severe corrosion damage was observed on the specimen surfaces of the sensitization-treated HNSSs, particularly the Mo-free HNSS A (Fig. 12a). The Mo alloying resulted in significant improvement on the corrosion resistance of the sensitization-treated HNSSs (Fig. 12b and c). The corrosion pits on the sensitization-treated specimen surfaces were much larger and deeper than those on the solution-annealed ones (Fig. 11b, c and 12b, c). It should be noted that intergranular attack also took place in the corrosion process of the sensitization-treated HNSSs in the $FeCl_3$ + HCl solution. Typical intergranular attack was observed to develop from the corrosion pits along the grain boundaries (Fig. 12d). This seemed to suggest that a synergy of pitting corrosion and intergranular attack dominated the corrosion behavior of the sensitization-treated HNSSs. In contrary to the HNSSs, the sensitization-treated 316L SS showed only typical inhomogenous corrosion pits without any intergranular attack on the specimen surface (Fig. 12e and f), just similar to the situation of the solution-annealed steel. The susceptibility of the present HNSSs and 316L SS to sensitization treatment closely depended on the chemical compositions of the steels, having been discussed in detail in our previous work (Ref 34). It is believed that a similar susceptibility to intergranular attack played a role during the electrochemical tests of the HNSSs and 316L SS in chloride solutions. As a result, both the polarization and EIS testing results showed that the sensitization treatment caused significant degradation on corrosion resistance of the HNSSs rather than the 316L SS.

5. Summary

The pitting corrosion behavior of three kinds of Ni-free and Mn-alloyed HNSSs and a 316L SS was investigated using electrochemical and immersion testing methods. Both the solution-annealed and sensitization-treated specimens were examined. The results are summarized as follows.

1. The solution-annealed HNSSs showed better pitting corrosion resistance than the solution-annealed 316L SS in both neutral and acidic NaCl solutions. The pitting potentials of the solution-annealed HNSSs were about 1 V higher than that of the 316L SS in acidic NaCl solutions. The addition of Mo seemed to have no further improvement on the pitting corrosion resistance of the solution-annealed HNSSs.
2. The critical current density for passivation of the solution-annealed HNSSs in acidic NaCl solution was larger than that of the 316L SS. The Mo alloying, to some extent, decreased the critical current density for passivation of the HNSSs. The larger critical current density for passivation of the HNSSs compared to the 316L SS could be attributed to accelerated anodic dissolution and/or selective dissolution of iron in acidic solution caused by Mn and N.
3. The sensitization treatment resulted in rapid degradation of corrosion resistance of the Mo-free HNSSs in both the neutral and acidic NaCl solutions. The pitting potential and the passive potential range of the sensitization-treated Mo-free HNSS significantly decreased in comparison with the solution-annealed steel, while the passive current

density increased significantly. The sensitization-treated HNSSs showed smaller polarization impedance values and more narrow capacitive loops compared to the solution-annealed steels. The addition of Mo remarkably improved the corrosion resistance of the sensitization-treated HNSSs. The pitting potential and the passive potential range of the sensitization-treated Mo-bearing HNSSs kept almost the same level as that of the solution-annealed steels in neutral and acidic NaCl solutions, but the passive current density of the sensitization-treated Mo-bearing HNSSs increased, particularly in neutral NaCl solution. The sensitization-treated Mo-bearing HNSSs had higher polarization impedance values and broader capacitive loops compared to the sensitization-treated Mo-free steel.

4. The solution-annealed 316L SS showed a larger pitting corrosion rate than the HNSSs in the $FeCl_3$ + HCl solution. Typical large size of corrosion pits appeared on the 316L SS specimen surface. The sensitization treatment caused the pitting corrosion rate of the HNSSs increased rapidly, particularly for the Mo-free HNSS. The intergranular attack was also found to take place in the pitting corrosion process for the sensitization-treated HNSSs, but not for the 316L SS.
5. The good resistance of the solution-annealed HNSSs to pitting corrosion could be attributed to the stable and protective passive film contributed by N, Cr, and Mo. The sensitization treatment degraded the passive film by decreasing the anti-corrosion elements and Cr-bearing oxides in the passive film.

Acknowledgments

This study was jointly supported by the Science and Technology Foundation of China (50534010) and the Innovation Fund of Institute of Metal Research (IMR), Chinese Academy of Sciences (CAS).

References

1. P.J. Uggowitzer, R. Magdowski, and M.O. Speidel, Nickel Free High Nitrogen Austenitic Steels, *ISIJ Int.*, 1996, **36**(7), p 901–908
2. M.O. Speidel and H.J. Speidel, Nitrogen Containing Austenitic Stainless Steels, *Proc. Inter. Conf. on High Nitrogen Steels 2006*, H. Dong, J. Su, and M. Speidel, Eds., Metallurgical Industry Press, Beijing. Jiuzhaigou Valley, China, August 2006, p 21–29
3. M. Sumita, T. Hanawa, and S.H. Teoh, Development of Nitrogen-Containing Nickel-Free Austenitic Stainless Steels for Metallic Biomaterials—Review, *Mater. Sci. Eng. C*, 2004, **24**(6–8), p 753–760
4. P.R. Levey and A.V. Bennekom, A Mechanistic Study of the Effects of Nitrogen on the Corrosion Properties of Stainless-Steels, *Corrosion*, 1995, **51**(12), p 911–921
5. H.J. Grabke, The Role of Nitrogen in the Corrosion of Iron and Steels, *ISIJ Int.*, 1996, **36**(7), p 777–786
6. H. Yashiro, D. Hirayasu, and N. Kumaga, Effect of Nitrogen Alloying on the Pitting of Type 310 Stainless Steel, *ISIJ Int.*, 2002, **42**(12), p 1477–1482
7. A.S. Vanini, J.P. Audouard, and P. Marcus, The Role of Nitrogen in the Passivity of Austenitic Stainless-Steels, *Corros. Sci.*, 1994, **36**(11), p 1825–1834
8. H. Baba, T. Kodama, and Y. Katada, Role of Nitrogen on the Corrosion Behavior of Austenitic Stainless Steels, *Corros. Sci.*, 2002, **44**(10), p 2393–2407
9. Y. Katada, N. Washizu, and H. Baba, Localized Corrosion Behavior of High Nitrogen Steel, *Mater. Sci. Forum*, 2005, **475–479**, p 225–228
10. H. Baba and Y. Katada, Effect of Nitrogen on Crevice Corrosion in Austenitic Stainless Steel, *Corros. Sci.*, 2006, **48**(9), p 2510–2524
11. S.D. Chyou and H.C. Shih, X-Ray Photoelectron Spectroscopy and Auger Electron Spectroscopy Studies on the Passivation Behavior of Plasma Nitrided Low-Alloy Steel in Nitric Acid, *Mater. Sci. Eng. A*, 1991, **148**(2), p 241–251
12. I. Olefjord and L. Wegrelius, The Influence of Nitrogen on the Passivation of Stainless Steels, *Corros. Sci.*, 1996, **38**(7), p 1203–1220
13. R. Bandy and D.V. Rooyen, Properties of Nitrogen Containing Stainless Alloy Designed for High Resistance to Pitting Corrosion, *Corrosion*, 1985, **41**(4), p 228–233
14. Y.C. Lu, R. Bandy, C.R. Clayton, and R.C. Newman, Surface Enrichment of Nitrogen During Passivation of a Highly Resistant Stainless Steel, *J. Electrochem. Soc.*, 1983, **130**(8), p 1774–1776
15. C.R. Clayton, G.P. Halada, and J.R. Kearns, Passivity of High Nitrogen Stainless Alloys—The Role of Metal Oxyanions and Salt Films, *Mater. Sci. Eng. A*, 1995, **198**(1–2), p 135–144
16. C.R. Clayton and R.G. Martin, Evidence of Anodic Segregation of Nitrogen in High Nitrogen Stainless Steels and Its Influence on Passivity, *Proc. Inter. Conf. on High Nitrogen Steels 1988*, J. Foct and A. Hendry, Eds., The Institute of Metals, London. Lille, France, May 1988, p 256–261
17. I. Olefjord and C.R. Clayton, Surface-Composition of Stainless-Steel During Active Dissolution and Passivation, *ISIJ Int.*, 1991, **31**(2), p 134–141
18. G.C. Palit, V. Kain, and H.S. Gadiyar, Electrochemical Investigations of Pitting Corrosion in Nitrogen Bearing Type 316LN Stainless Steel, *Corrosion*, 1993, **49**(12), p 977–991
19. R.C. Newman and M.A.A. Ajjawi, A Micro-Electrode Study of the Nitrate Effect on Pitting of Stainless Steels, *Corros. Sci.*, 1986, **26**(12), p 1057–1063
20. Y.C. Lu and M.B. Ives, Inhibition of Transpassive Reactions of Molybdenum by Nitriding, *Corros. Sci.*, 1992, **33**(2), p 317–320
21. Y.C. Lu, M.B. Ives, and C.R. Clayton, Synergism of Alloying Elements and Pitting Corrosion Resistance of Stainless Steels, *Corros. Sci.*, 1993, **35**(1–4), p 89–96
22. C.O.A. Olsson, The Influence of Nitrogen and Molybdenum on Passive Films Formed on the Austenoferritic Stainless Steel 2205 Studied by AES and XPS, *Corros. Sci.*, 1995, **37**(3), p 467–479
23. R.C. Newman and T. Shahrabi, The Effect of Alloyed Nitrogen or Dissolved Nitrated Ions on the Anodic Behavior of Austenitic Stainless Steel in Hydrochloric Acid, *Corros. Sci.*, 1987, **27**(8), p 827–838
24. H. Ezuber, A.J. Betts, and R.C. Newman, *Mater. Sci. Forum*, 1989, **44/45**, p 247
25. R.C. Newman, Y.C. Lu, R. Bandy, and C.R. Clayton, Mechanism of Passivation in Stainless Steels Containing High Concentrations of Nitrogen, *Proc. 9th Int. Conf. Metallic Corrosion*, Toronto, Canada, 1984. National Research Council, Ottawa, p 394–398
26. G.P. Halada, C.R. Claton, D. Kim, and J.R. Kearns, Electrochemical and Surface Analytical Studies of the Interaction of Nitrogen with Key Alloying Elements in Stainless Steels, *NACE/Corrosion*, 1995, paper no. 531
27. M.J. Czachor, E. Lunarska, and Z.S. Smialowska, Effect of Nitrogen Content in a 18Cr-5Ni-10Mn Stainless Steel on the Pitting Susceptibility in Chloride Solutions, *Corrosion*, 1975, **31**(11), p 394–398
28. R. Bandy and D.V. Rooyen, Pitting Resistant Alloys in Highly Concentrated Chloride Media, *Corrosion*, 1983, **39**(6), p 227–236
29. R.F.A. Jargelius-Pettersson, Application of the Pitting Resistance Equivalent Concept to Some Highly Alloyed Austenitic Stainless Steels, *Corrosion*, 1998, **54**(2), p 162–168
30. K. Zagorski and A. Doraczynska, Potentiodynamic Polarization Behavior of Two 17Cr-13Ni-2.5Mo Steels with different N Contents, *Corros. Sci.*, 1976, **16**(6), p 405–450
31. I. Betova, M. Bojinov, T. Laitinen, K. Makela, P. Pohjanne, and T. Saario, The Transpassive Dissolution Mechanism of Highly Alloyed Stainless Steels I. Experimental Results and Modelling Procedure, *Corros. Sci.*, 2002, **44**(12), p 2675–2697
32. H.H. Lee and H.H. Uhlig, Effect of Nickel in Cr-Ni Stainless Steels on the Critical Potential for Stress Corrosion Cracking, *J. Electrochem. Soc.*, 1970, **117**(1), p 18–22
33. J. Menzel, W. Kirschner, and G. Stein, High Nitrogen Containing Ni-Free Austenitic Steels for Medical Applications, *ISIJ Int.*, 1996, **36**(7), p 893–900

34. X.Q. Wu, S. Xu, J.B. Huang, E.H. Han, W. Ke, K. Yang, and Z.H. Jiang, Uniform and Intergranular Corrosion Behavior of Nickel Free and Manganese Alloyed High Nitrogen Stainless Steels, *Mater. Corros.*, 2008, **59**. doi:10.1002/maco.200804102
35. R.J. Brigham and E.W. Tozer, Localized Corrosion Resistance of Mn-Substituted Austenitic Stainless Steels: Effect of Molybdenum and Chromium, *Corrosion*, 1976, **32**(7), p 274–276
36. Y.S. Lim, J.S. Kim, S.J. Ahn, H.S. Kwon, and Y. Katada, The Influences of Microstructure and Nitrogen Alloying on Pitting Corrosion of Type 316L and 20 wt.% Mn-Substituted Type 316L Stainless Steels, *Corros. Sci.*, 2001, **43**(1), p 53–68
37. B.R. Tzaneva, L.B. Fachikov, and R.G. Raicheff, Pitting Corrosion of Cr-Mn-N Steel in Sulphuric Acid Media, *J. Appl. Electrochem.*, 2006, **36**(3), p 347–353
38. K. Sugimoto and Y. Sawada, The Role of Molybdenum Addition to Austenitic Stainless Steels in the Inhibition of Pitting in Acid Chloride Solutions, *Corros. Sci.*, 1977, **17**(5), p 425–445
39. M. Urquidi-Macdonald and D.D. Macdonald, Theoretical Analysis of the Effects of Alloying Elements on Distribution Functions of Passivity Breakdown, *J. Electrochem. Soc.*, 1989, **136**(4), p 961–967
40. C.O.A. Olsson and D. Landolt, Film Growth During Anodic Polarization in the Passive Region on 304 Stainless Steels with Cr, Mo, or W Additions Studied with EQCM and XPS, *J. Electrochem. Soc.*, 2001, **148**(11), p B438–B449
41. J.M. Bastidas, C.L. Torres, E. Cano, and J.L. Polo, Influence of Molybdenum on Passivation of Polarised Stainless Steels in a Chloride Environment, *Corros. Sci.*, 2002, **44**(3), p 625–633
42. F.E.T. Heakal, A.A. Ghoneim, and A.M. Fekry, Stability of Spontaneous Passive Films on High Strength Mo-Containing Stainless Steels in Aqueous Solutions, *J. Appl. Electrochem.*, 2007, **37**(3), p 405–413
43. M.G. Pujar, N. Parvathavarthini, and R.K. Dayal, Some Aspects of Corrosion and Film Formation of Austenitic Stainless Steel Type 316LN Using Electrochemical Impedance Spectroscopy (EIS), *J. Mater. Sci.*, 2007, **42**(12), p 4535–4544
44. R.D. Armstrong and K. Edomondson, The Impedance of Metals in the Passive and Transpassive Regions, *Elecctrochim. Acta*, 1973, **18**(12), p 937–943
45. J.L. Polo, E. Cano, and J.M. Bastidas, An Impedance Study on the Influence of Molybdenum in Stainless Steel Pitting Corrosion, *J. Electroanal. Chem.*, 2002, **537**(1–2), p 183–187
46. S.J. Pawel, E.E. Stansbury, and C.D. Lundin, Role of Nitrogen in the Pitting Resistance of Cast Duplex CF-Type Stainless Steels, *Corrosion*, 1989, **45**(2), p 125–133
47. R.D. Willenbruch, C.R. Clayton, M. Oversluizen, D. Kim, and Y. Lu, An XPS and Electrochemical Study of the Influence of Molybdenum and Nitrogen on the Passivity of Austenitic Stainless Steel, *Corros. Sci.*, 1990, **31**(1), p 179–195
48. Y.C. Lu, J.L. Luo, and M.B. Ives, Effect of Nitriding on the Anodic Behavior of Iron and Its Significance in Pitting Corrosion of Iron-Based Alloys, *Corrosion*, 1991, **47**(11), p 835–839
49. G.P. Halada, D. Kim, and C.R. Clayton, A Surface analytical Study of the Influence of Nitrogen on the Electrochemical Passivation of High Ni Stainless Steels and Thin Mo-Ni Films, *NACE/Corrosion*, 1995, paper no. 536